

A Proposal for a Parameterized Circulating Vector Field Guidance for Fixed Wing
Unmanned Aerial Vehicles

A thesis presented to
the faculty of
the Russ College of Engineering and Technology of Ohio University

In partial fulfillment
of the requirements for the degree
Master of Science

Garrett S. Clem
December 2017
© 2017 Garrett S. Clem. All Rights Reserved.

This thesis titled

A Proposal for a Parameterized Circulating Vector Field Guidance for Fixed Wing
Unmanned Aerial Vehicles

by

GARRETT S. CLEM

has been approved for

the Department of Mechanical Engineering

and the Russ College of Engineering and Technology by

Jay P. Wilhelm

Assistant Professor of Mechanical Engineering

Dennis Irwin

Dean, Russ College of Engineering and Technology

ABSTRACT

CLEM, GARRETT S., M.S., December 2017, Mechanical Engineering

A Proposal for a Parameterized Circulating Vector Field Guidance for Fixed Wing

Unmanned Aerial Vehicles (35 pp.)

Director of Thesis: Jay P. Wilhelm

ABSTRACT

DED

ACKNOWLEDGMENTS

ACK

TABLE OF CONTENTS

	Page
Abstract	3
Dedication	4
Acknowledgments	5
List of Tables	7
List of Figures	8
List of Symbols	9
List of Acronyms	10
 1 Introduction	11
1.1 Motivation and Problem Statement	11
1.2 Methods Overview	12
1.3 Phase I	12
1.4 Phase II	12
1.5 Phase III	12
1.6 Summary of Phases	13
 2 Literature Review	14
2.1 Introduction to Literature Review	14
2.2 Fixed Wing Unmanned Aerial Vehicle	14
2.2.1 Introduction to Fixed Wing UAV	14
2.2.2 Autopilot and Ground Station	15
2.3 Vector Field Guidance	18
2.3.1 Introduction to Vector Field Guidance	18
2.3.2 Potential Field	18
2.3.3 Virtual Force Field - Histogram Method	21
2.3.4 Lyapunov Vector Fields	22
2.3.5 Non-Lyapunov Vector Fields	25
2.3.6 Gradient Vector Field	26
2.4 Unmanned Aerial Vehicle Simulation	32
2.5 Literature Review Summary	33
 References	34

LIST OF TABLES

Table	Page
-------	------

LIST OF FIGURES

Figure	Page
2.1 Hand Launched Fixed Wing UAV and Global Hawk	14
2.2 Autopilot Navigation Guidance and Control	16
2.3 Pixhawk Autopilot	16
2.4 Unmanned Aerial System	17
2.5 Single Obstacle Potential Field Gradient [5]	19
2.6 Potential Field Local Minimum [5]	20
2.7 Obstacle Clustering [5]	20
2.8 Virtual force field histogram acting on a mobile robot	21
2.9 Lyapunov vector field for straight line and circular primitives	22
2.10 Lyapunov vector field approach curved path asymptotically	23
2.11 Elliptical VF produced by non-linear coordinate transformations a) [11] b) [12]	24
2.12 Tangent plus lyapunov vector fields for shortest path target tracking [14]	24
2.13 RRT* path planner with a VF used as a task specification	25
2.14 Vector field within a set of constrained delaunay triangles [16]	26
2.15 Attractive vector field (a) and clockwise circulation field (b)	27
2.16 Repulsive vector field a) and counterclockwise circulation field b)	28
2.17 Place holder image of UAV following ground target	28
2.18	29
2.19	30
2.20 Dubins UAV actuator saturation	31
2.21 Differential drive mobile robot simulating fixed wing UAV Dubins constraints	32

LIST OF SYMBOLS

a Previous or Initial Axial Induction Factor (-)

LIST OF ACRONYMS

AoA Angle of Attack

1 INTRODUCTION

1.1 Motivation and Problem Statement

Fixed wing Unmanned Aerial Vehicles are used for long endurance missions such as surveillance that would fatigue pilots or put them in harms way [1]. Missions are typically built using waypoint navigation and loitering executed by path following [2]. Obstacles are not always known during path planning and once discovered, a new path must be generated. Planning obstacle free and flyable paths takes time and may be impossible to relay to a UAV if communication is not reliable. Guidance that follows mission paths while avoiding obstacles without the need for constant communication with a ground station may be beneficial. Gradient Vector Fields (GVF) produce heading guidance at any point in space by summing together convergence and circulation field components. Each component uses a static scalar weight. Obstacles have been represented as separate repulsive GVFs that are later summed to the path following GVF [Wilhelm, Wambold, Clem]. Static GVF weights do not consider the state of the UAV resulting in sub-optimal guidance. Modifying the GVF convergence and circulation weights to be functions of common UAV states may generate an optimal guidance. **The proposed research seeks to determine GVF weighting functions that construct optimal obstacle avoidance.**

1.2 Methods Overview

The proposed research will be conducted in three phases where singularities will be demonstrated, weighting functions will be investigated, and a developed GVF will be validated on a ground robot simulating a UAV. Phases I and II will be conducted in a simulation environment that combines mission paths and obstacles into a single GVF. Phase III will be conducted with a ground robot simulating a UAV guided by the modified GVF in real-time. Dubins fixed wing constraints will be imposed in simulations and experiments.

1.3 Phase I

Recreate vector fields for circular and elliptical obstacles and demonstrate singularities. A simulation environment will be built that generates GVFs consisting of mission paths and obstacles. Circular and elliptical obstacles will be investigated and the resulting singularities will be characterized. Static weights will be used and the performance of the guidance measured in distance traveled and time of flight.

1.4 Phase II

Investigate GVF weighting functions that influence obstacle avoidance. UAV closing rate, position, and range will be used to develop dynamic GVF weights for convergence and circulation. The modified GVF will be compared against a static and strictly repulsive GVF. Distance traveled and time of flight will be used to compare the modified GVF to the unmodified GVF.

1.5 Phase III

Validate modified GVF model with ground robot experiments. The modified GVF developed in Phase II will be implemented on a differential drive ground robot simulating a fixed wing UAV. Guidance to guide the robot to a path while avoiding static obstacles will be demonstrated.

1.6 Summary of Phases

Each phases consists of a **goal** that will be accomplished by executing *objectives*. Completion of all objectives and phases will result in the final deliverable.

Phase I: Demonstrate Gradient Vector Field Singularities

1. *Build a GVF simulation environment*
2. *Derive GVF for circular and elliptical obstacles*
3. *Identify path and obstacles where singularities are produced*

Phase II: Investigate GVF weighting functions that influence obstacle avoidance

1. *Formulate circulation and convergence weights as functions of UAV state*
2. *Determine combination of GVF weights that produces optimal guidance in simulation*

Phase III: Validate modified GVF model with ground robot experiments

1. *Build differential drive robot*
2. *Build robotic framework to take guidance commands*
3. *Repeat simulations performed in Phase II on ground robot*

Deliverable: Modified GVF optimal guidance for path following and static obstacle avoidance.

2 LITERATURE REVIEW

2.1 Introduction to Literature Review

2.2 Fixed Wing Unmanned Aerial Vehicle

2.2.1 Introduction to Fixed Wing UAV

Unmanned Aerial Vehicles (UAVs) operate without an on-board pilot making them ideal for high endurance and dangerous missions. Remotely piloted aircraft can trade-off pilots when they become fatigued allowing the aircraft to remain in service for longer periods of time. UAVs do not have cockpits or life support systems which free up space for additional equipment and reduces costs. The lack of an on-board pilot and low system costs also allows a UAV to be expendable. UAVs can be found in rotorcraft and fixed wing varieties. Fixed wing UAVs range widely in form factor and size, but typically fall under either hand-launched or large systems. Hand launched varieties can be carried on the back of a soldier and launched without the use of a runway and are typically battery powered. Large fixed wing UAVs are typically gas powered and require a runway to take-off and land.



(a)



(b)

Figure 2.1: Hand Launched Fixed Wing UAV and Global Hawk

Hand-launched UAVs are primarily tasked with surveilling the immediate area for soldiers on the ground. Cameras on-board relay video to the ground allowing soldiers to identify threats prior to engagement. Large UAVs are tasked with surveillance and can be used for armed reconnaissance [1]. Missions can be described in terms of a path that a UAV is required to fly on. The paths are typically constructed from simple primitives such as straight lines connecting waypoints and circular loiter paths. Obstacle free and flyable paths are generated at a ground station prior to flight and sent to the UAV. The UAVs autopilot uses the path as a reference and attempts to keep the UAV as close to the path as possible. The relationship between a ground station and a UAV is discussed in more detail in the following section.

2.2.2 Autopilot and Ground Station

Autopilots are devices that control the position and attitude of a UAV by implementing guidance, navigation, and control systems. Accelerometers, gyroscopes, barometers, and compasses measure the state of a UAV and are passed to the navigation system. Measurements are often noisy and need to be fused together which is commonly done with a kalman filter [3]. The state estimates are used as feedback for both the guidance and control systems, depicted in Figure 2.2. Sensor uncertainty and wind disturbances cause the UAV to deviate from the reference path over time and needs to be corrected. The guidance system compares the estimated state of a UAV to the reference path and provides guidance commands in the form of a heading to the control system. State estimates are also fed into the control system as feedback along with guidance commands to produce pulse width modulation commands to actuators. The actuators produce a physical output that alters the state of the UAV which is again measured and estimated by the navigation system.

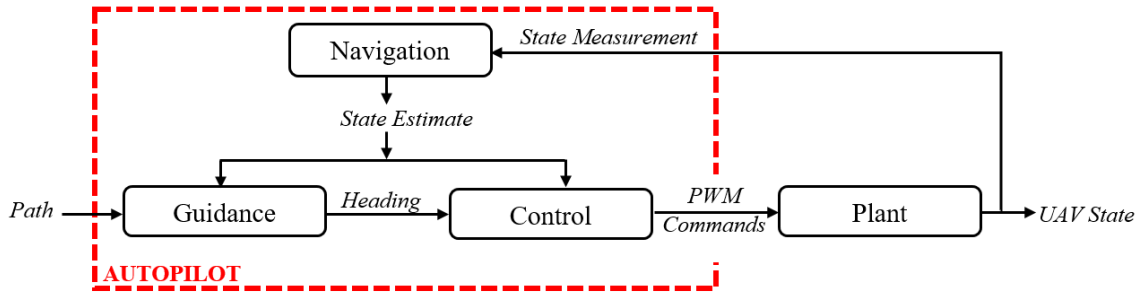


Figure 2.2: Autopilot Navigation Guidance and Control

A typical autopilot is shown in Figure 2.3 which is programmed with navigation, guidance, and control software. Accelerometers, gyroscopes, barometers and the compass are included inside the autopilot and makeup the inertial measurement unit (IMU). Additional sensors such as GPS and airspeed sensors can be connected as peripheral devices. Radios are connected to receive transmitter commands and communicate with a ground station.



Figure 2.3: Pixhawk Autopilot

Ground stations are computers that run mission management software that allow users to configure vehicles and program missions. Missions are planned at the ground station where high level mission objectives are assigned to points on a map such as waypoints and loitering maneuvers. Ground station software generates obstacle free and flyable paths that connect mission objectives and relay paths to the autopilot over radio link.

Information collected by the UAV can be relayed back to the ground station for analysis. Transmitters can be used to control the UAVs movements directly. Ground stations and autopilots work together to form an Unmanned Aerial System (UAS) depicted in Figure 2.4.



Figure 2.4: Unmanned Aerial System

Once paths have been generated, such as that shown in Figure ??, they are sent to the UAV via radio link. The guidance system is then responsible for guiding the UAV to get on and follow the path. Common methods for guiding algorithms for getting on and following a path include carrot chasing, non-linear guidance law (NLGL), pure pursuit line of sight (PLOS), linear quadratic regulator (LQR) and vector field [2]. Benchmarks for how each guidance algorithm performs is commonly quantified in control effort and tracking error with respect to the reference path. Sujit et al. compared the above guidance laws and discussed the benefits and disadvantages of the guidance laws, and in terms of control effort and tracking error LQR and vector field performed the best respectively. LQR was shown

to have optimal control effort but exhibited large cross track error when subjected to high wind speeds. Vector field produced guidance with the lowest tracking error but experienced osculations once on the path.

2.3 Vector Field Guidance

2.3.1 Introduction to Vector Field Guidance

Vector field is a continuous guidance and control method that applies artificial attractive and repulsive forces to a point mass. The two broad categories of algorithms that produce vector fields consist of potential field algorithms and path following algorithms. Potential field produces guidance and control to a robot for converging to a distinct point. Path following algorithms produce guidance for converging and following a path. Several path following vector field algorithms have been investigated including gradient vector field, which provides convenient convergence and circulation weights that may be useful for providing an optimal guidance for obstacle avoidance.

2.3.2 Potential Field

Potential field was introduced as a real-time robotic manipulator algorithm for obstacle avoidance [4]. The potential field algorithm represents a robots workspace as a gradient potential of attractive and repulsive artificial forces that drive the robot to a desired goal. Goals are given the lowest potential and act as attractive forces. Obstacles have high potential and act as repulsive forces. A simple example is depicted in Figure 2.5 consisting of an initial state, a goal, and a single obstacle. The initial state of the robot is at the edge of a gradient where the potential is maximum. In the lowest part of the gradient a goal exists at the global minimum. Obstacles are added to the potential field, but have limited effect due to a decay function.

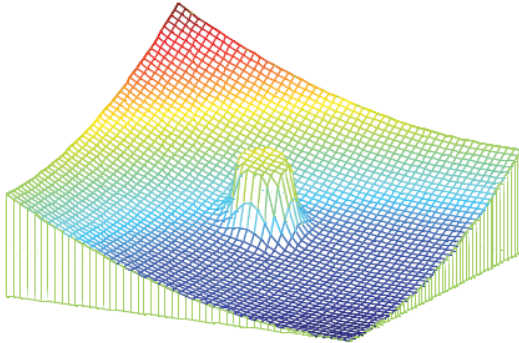


Figure 2.5: Single Obstacle Potential Field Gradient [5]

Potential field is unique in that path planning, trajectory planning, and control are lumped into a single system [6]. Transition from an initial state to a goal state traditionally occurred by executing three steps consisting of path planning, trajectory planning, and control. Path planning dealt with finding an obstacle free path from an initial state to a goal state. Trajectory planning time parametrized the obstacle free path with some high level vehicle constraints considered. Lastly, control attempts to reduce the tracking error with respect to the reference trajectory. Combining the three motion planning steps into a single algorithm has been shown to be computational inexpensive [7].

As pointed out in [8], robots using potential field are susceptible to local minimum. Encountering a local minimum prevents the robot from continuing down the gradient and into the global minimum because equilibrium has been reached prematurely. Figure 2.6 demonstrates local minimum by adding several obstacles into a goal field. Several methods have been developed to mitigate the effects of local minimums as pointed out in [7] through the use of navigation functions. Local minimum produced as a result of closely spaced obstacles as shown in Figure 2.6 have been addressed by grouping obstacles together into a cluster [5].

Several methods have been developed to mitigate the effects of local minimums as pointed out in [7] through the use of navigation functions. Local minimum produced

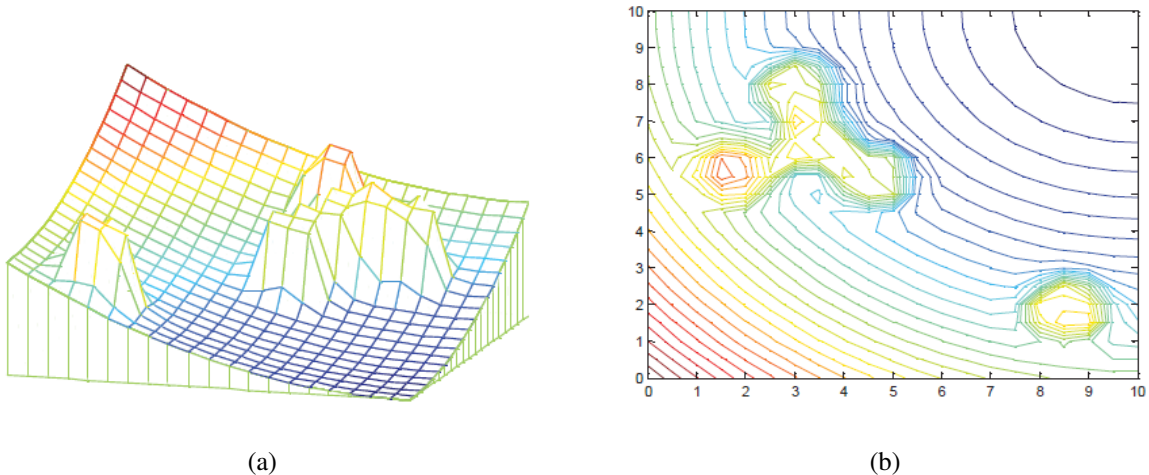


Figure 2.6: Potential Field Local Minimum [5]

as a result of closely spaced obstacles as shown in Figure 2.6 have been addressed by grouping obstacles together into a cluster [5]. Grouping obstacles addresses the risk of local minima before forming the potential field. If local minima are encountered after the field is generated, additional forces can be applied to push the robot away from the local minima.

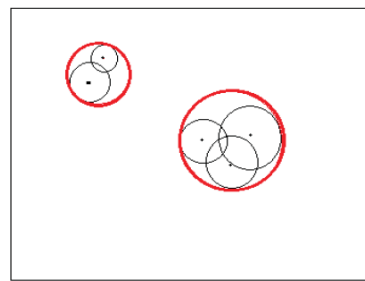


Figure 2.7: Obstacle Clustering [5]

Potential fields ability to avoid obstacles and combine path planning, trajectory planning, and control into a single system while being computationally inexpensive makes it an attractive option for many robotic systems. Fixed wing UAVs must maintain a

minimum forward velocity and cannot converge to a single point, making potential field difficult to implement.

2.3.3 Virtual Force Field - Histogram Method

When the environment changes, such as a new obstacle or the goal has moved, the potential field has to be recalculated. Koren and Borenstein developed a virtual force field (VFF) histogram method that guides a mobile robot to a known goal while avoiding initially unknown obstacles [8]. VFF decomposes a robots workspace into discretized cells that contain an integer certainty value associated with the confidence that an obstacle occupies the cell. A global goal applies an artificial attractive force on the robot that pulls it closer to the goal. As the robot detects obstacles, the certainty value increases in the cell associated with the obstacles position. Cells apply artificial repulsive forces with magnitudes that depend on the certainty value and the distance to the cell.

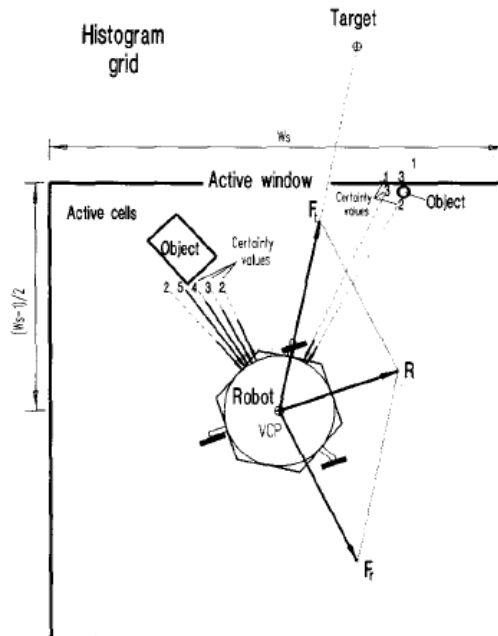


Figure 2.8: Virtual force field histogram acting on a mobile robot

The VFF histogram method was validated on a mobile robot platform using ultrasonic sensors in [8] and [9], avoiding obstacles and seeking a goal. Certainty cells in VFF only provide strictly repulsive vectors which guide the robot away, but provide no guidance for getting around the obstacle.

2.3.4 Lyapunov Vector Fields

Fixed wing UAVs must maintain a minimum forward velocity therefore cannot converge to a single point making potential field or VFF guidance difficult. Missions for UAVs are typically constructed from obstacle free paths build from straight line and circular arc primitives. Path planning provides a reference to the autopilot that guides the UAV to first arrive at and subsequently follow the desired path while under the influence of external disturbances. Arriving at and following the path are typically achieved by generating vectors normal and parallel to the path respectively. Nelson et al. introduced a vector field generation method for straight line and circular arcs using Lyapunov stability arguments [10] and is depicted in Figure 2.9.

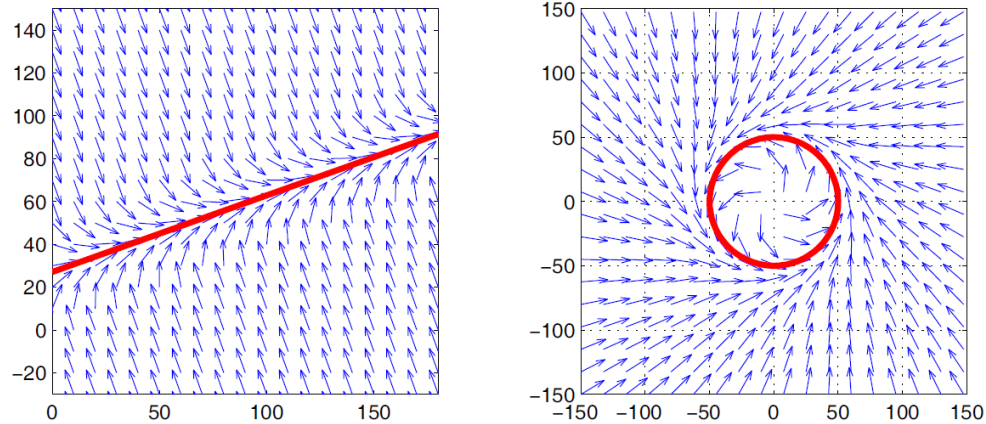


Figure 2.9: Lyapunov vector field for straight line and circular primitives

To construct flyable paths out of the primitives, it was necessary to determine how the resulting vector fields should be combined. Summing the fields directly result in **dead-zones, sinks, and singularities**. The solution was to have a single field active at any time, switching when the UAV reached the end of a primitive. Nelson's method was extended by Griffiths for curved path following and showed that the vectors asymptotically approach the curved path, shown in Figure 2.10.

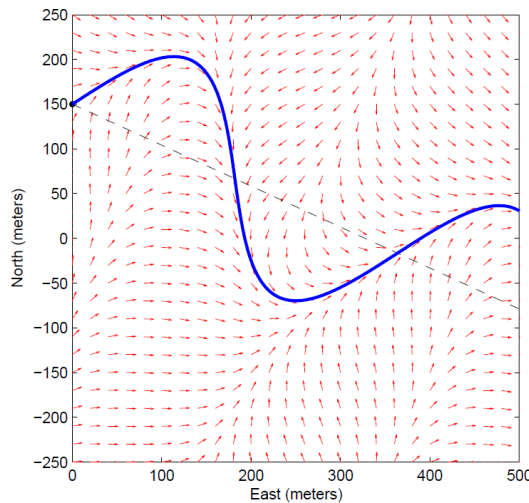


Figure 2.10: Lyapunov vector field approach curved path asymptotically

Primitive circular fields can be modified via non-linear coordinate transformations to produce globally convergent elliptical fields [11] [12]. Frew simulated and experimentally validated the transformed vector field where multiple fixed wing UAVs cooperatively tracked a moving target while maintaining a staggered distance from each other, preventing collision and multiple surveillance angles. The location of a target being tracked is not known with absolute certainty. The covariance matrix from a kalman filter to transform a circular vector field around an uncertain target was investigated in [12] and an example field is shown in Figure 2.11b.

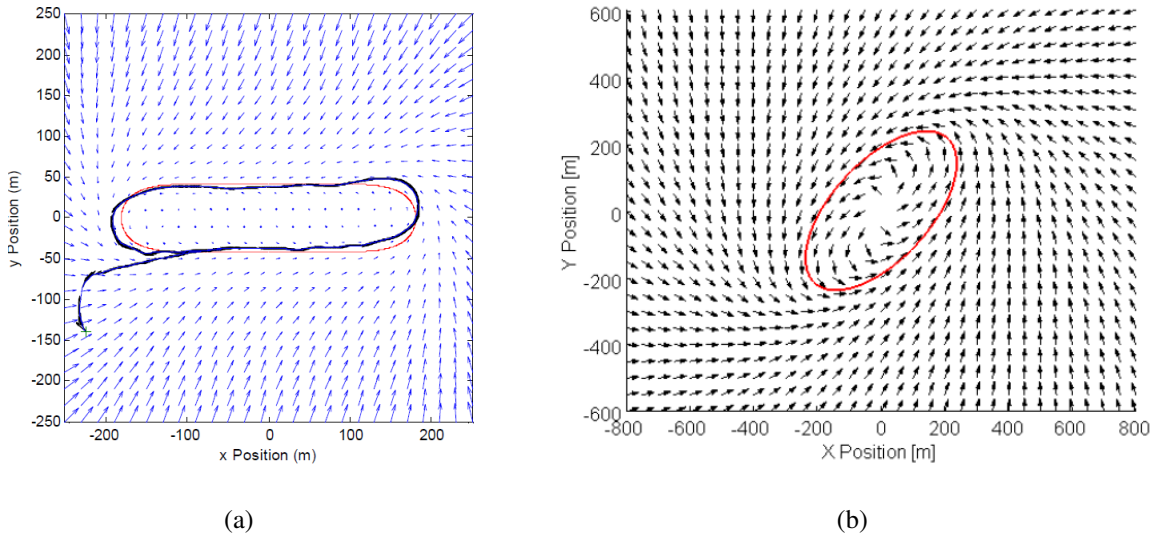


Figure 2.11: Elliptical VF produced by non-linear coordinate transformations a) [11] b) [12]

A target tracking lyapunov plus tangent vector field was introduced in [13] that produced shorter paths compared to lyapunov alone. Outside of the standoff circle, tangent vectors were said to provide the shortest distance to the circle. Inside the standoff circle, no tangent lines exist and lyapunov is used in its place. Figure 2.12 shows the difference in paths taken for lyapunov and tangent vector fields outside the standoff circle. The TPLVF was later used for path planning to avoid obstacles in [14].

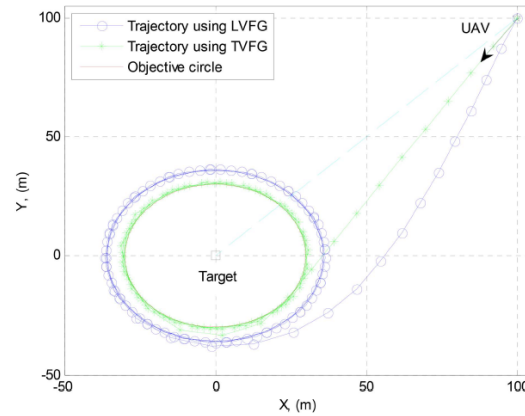


Figure 2.12: Tangent plus lyapunov vector fields for shortest path target tracking [14]

2.3.5 Non-Lyapunov Vector Fields

All methods that consider obstacles so far build a vector field that guides the UAV to an obstacle free path. Another approach is to build a vector field tending to a path and use optimal rapid random trees (RRT*) to explore the space for obstacles and select the optimal path. Pereia et al. developed such a method that builds a tree that makes up possible paths for the UAV to take. Branches extend from the root, or initial location of the UAV, randomly throughout the map with a constrained deviation from the initial vector field. When a branch encounters an obstacle it is trimmed and no longer explored. The path of minimum cost, or least distance, is selected for the UAV to use as a reference path. An example of the algorithm is shown in Figure 2.13.

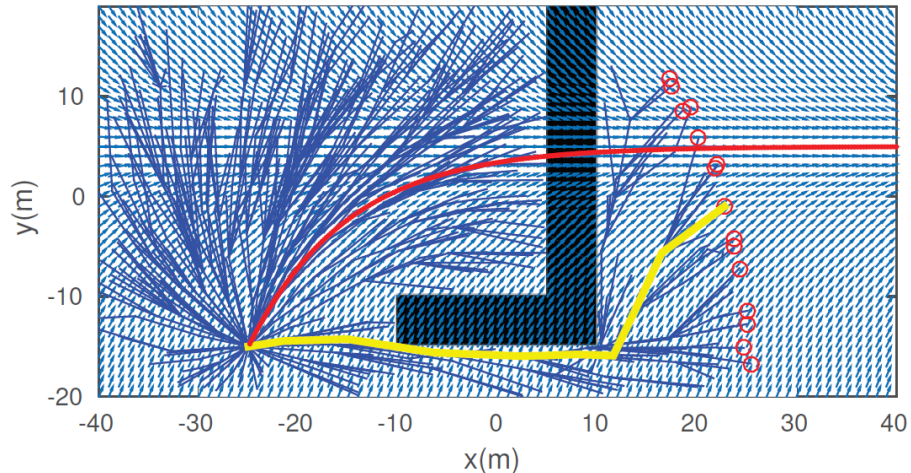


Figure 2.13: RRT* path planner with a VF used as a task specification

For well known obstacles in urban environments, such as buildings, an optimal path can be constructed with constrained delaunay triangulation (CDT) which has been previously used in computer animation [15]. CTD was used to construct vector fields in [16] that restricts robots movements inside the triangles while moving towards a global

goal. A simulation of a robot traversing a vector field inside a set of CDTs can be seen in Figure 2.14.

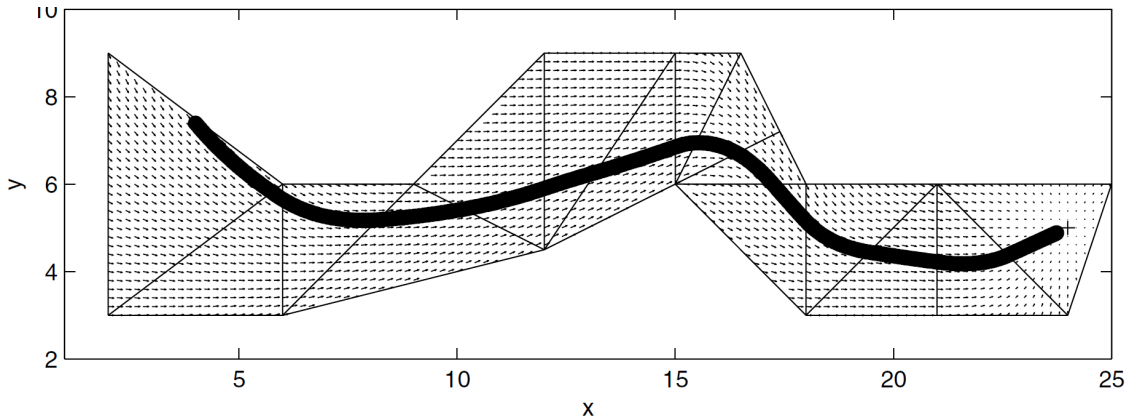


Figure 2.14: Vector field within a set of constrained delaunay triangles [16]

So far all of the vector field methods discussed have avoided obstacles by planning paths around them. Paths are typically calculated at the ground station and if communication is lost a new path may not be relayed to a UAV encountering a new obstacle. A possible solution is using vector fields to provide a repulsive force, not unlike the VFF method, immigrating around the obstacle.

2.3.6 Gradient Vector Field

The gradient vector field method was first introduced in [17] and produces an n -dimensional vector field guaranteed to converge to a path made of points that lie at the intersection of two surfaces. The total vector field \vec{V} is produced by summing together a convergence, circulation, and time varying terms seen in Equation ???. Convergence terms contribute vectors normal to the path, circulation terms contribute vectors parallel to the path, and time varying vectors account for changes in the path as a function of time.

$$\vec{V} = \mathbf{G}\vec{V}_{conv} + \mathbf{H}\vec{V}_{circ} + \mathbf{L}\vec{V}_{tv} \quad (2.1)$$

Each term is multiplied by a scalar, \mathbf{G} , \mathbf{H} , \mathbf{L} , that weights the contribution of each term on the total field \vec{V} . Only static paths will be discussed so it is assumed the time varying field is null. The advantage of GVF is the convenient access to the weighting terms that independently effect the total field. Magnitude of the weights modifies the strength of each fields influence, whereas the sign indicates the direction. Figure 2.15 shows convergence and circulation fields for a circular path where the weights \mathbf{G} and \mathbf{H} are unity and positive. The convergence field contains vectors that are normal to the circular path for all points in space, with exception to the center of the circle which is undefined. Circulation fields contain vectors that are parallel to the path for all points in space with the same exception of no definition at the center of the circle.

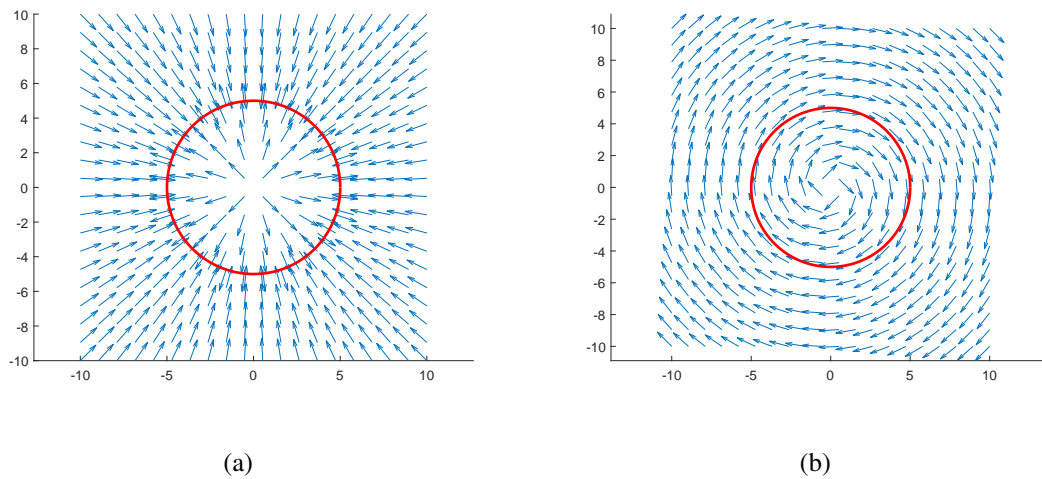


Figure 2.15: Attractive vector field (a) and clockwise circulation field (b)

Modifying the signs of \mathbf{G} and \mathbf{H} to be unity and negative results in similar fields but with a 180° rotation about the center of the circle, Figure 2.16. The attractive convergence field becomes a repulsive field, where all vectors are anti-normal to the path. The circulation field changes direction and rotates counterclockwise around the path.

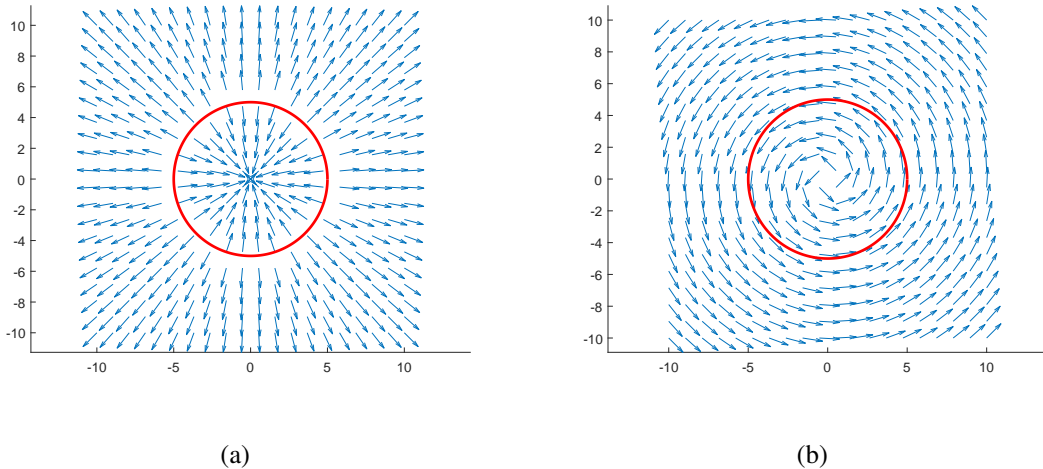


Figure 2.16: Repulsive vector field a) and counterclockwise circulation field b)

Repulsive fields have been used for obstacle avoidance for a UAV loitering around a moving target in [w,w,c]. A circular goal path was attached to a ground vehicle and a convergence and circulation vector field was generated. Circular paths were with small radii were placed on top of obstacles with strictly repulsive weights. Notice in Figure 2.16a that inside of the path, vectors guide inward, which is not desired for obstacle avoidance. The problem is alleviated by reducing the radius significantly. Goal and obstacle field are summed together to provide a total field that provides guidance to a UAV. Loitering is accomplished while avoiding two obstacles, as shown in Figure 2.17

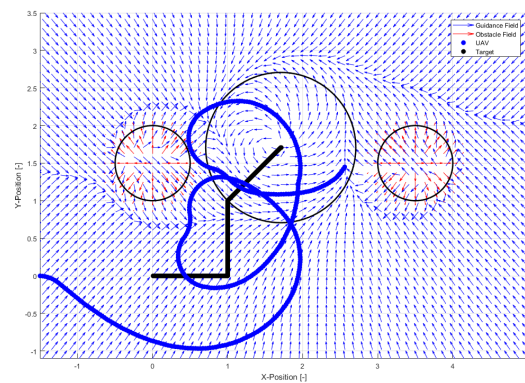


Figure 2.17: Place holder image of UAV following ground target

Similar to potential field and VFF, the strength of the repulsive field depends on the distance from an obstacle. In [w,w,c], a tangent hyperbolic decay function was assigned to the obstacle fields which varied the total strength from null to unity, shown in Figure 2.18.

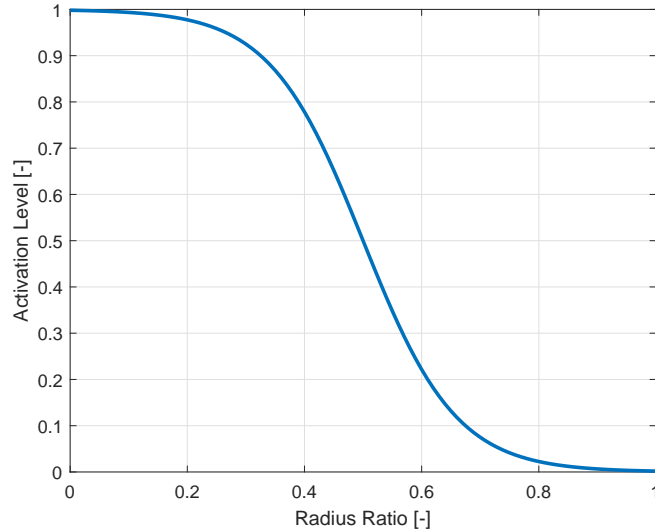


Figure 2.18:

Constructing the paths for a UAV flying at constant altitude requires three-dimensional surfaces intersecting to form two-dimensional paths. Consider a UAV in 2-dimensional space tracking a path τ , which is made of points that lie at the intersection of two surfaces. Each of the surfaces α_i is continuous, differentiable, and is a function of the set $q = [x, y, z]$. The convergence field \vec{V}_{conv} is produced by the sum of surfaces multiplied by their respective partial gradient $\nabla_q \alpha_i$. The definition of the convergence field is summarized in Equations 2.2 and 2.3.

$$\vec{V}_{conv} = \mathbf{G} \sum_{i=1}^{n-1} \alpha_i \nabla_q \alpha_i \quad (2.2)$$

$$\nabla_q = \begin{bmatrix} \frac{\partial}{\partial x} \\ \frac{\partial}{\partial y} \\ \frac{\partial}{\partial z} \end{bmatrix} \quad (2.3)$$

To produce a circular path of radius r the intersection of a cylinder and plane are used, as shown in Equations 2.4-2.5 and pictured in Figure 2.19.

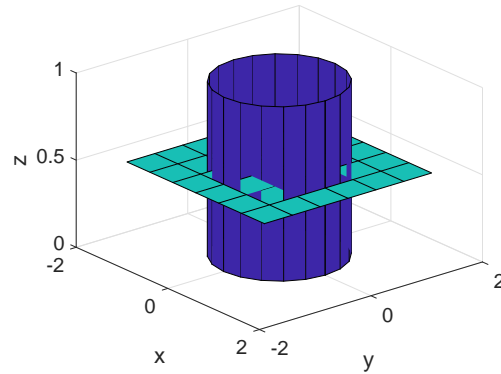


Figure 2.19:

$$\alpha_1 = x^2 + y^2 - r^2 \quad (2.4)$$

$$\alpha_2 = z \quad (2.5)$$

Convergence vector field term is produced by taking the wedge product of the partials $\nabla_q \alpha_i$, which in three dimensions simplifies to the cross product as shown in Equations 2.6 and 2.7.

$$\vec{V}_{circ} = \mathbf{H} \wedge_{i=1}^{n-1} \nabla_q \alpha_i \quad (2.6)$$

$$\vec{V}_{circ} = \mathbf{H} (\nabla_q \alpha_1 \times \nabla_q \alpha_2) \quad (2.7)$$

Circulation and convergence terms may have different magnitudes depending on the location of origin of a vector and the equations used for surfaces. Normalizing each component prior to weighting allows for more predictable results when assigning values. So far the VF weights have been used for high level specification of the desired behavior for a UAV, whether it be for convergence, avoidance, or circulation. Furthermore, there is no guarantee that when using a vector field for avoidance that the UAV will not violate the no-fly zone. If the UAV turn rate is at saturation an increased reference command will do nothing to aid in avoidance. A demonstration of saturation is seen in Figure 2.20 where a UAV is provided guidance by a convergent and circulating vector field about a circular path.

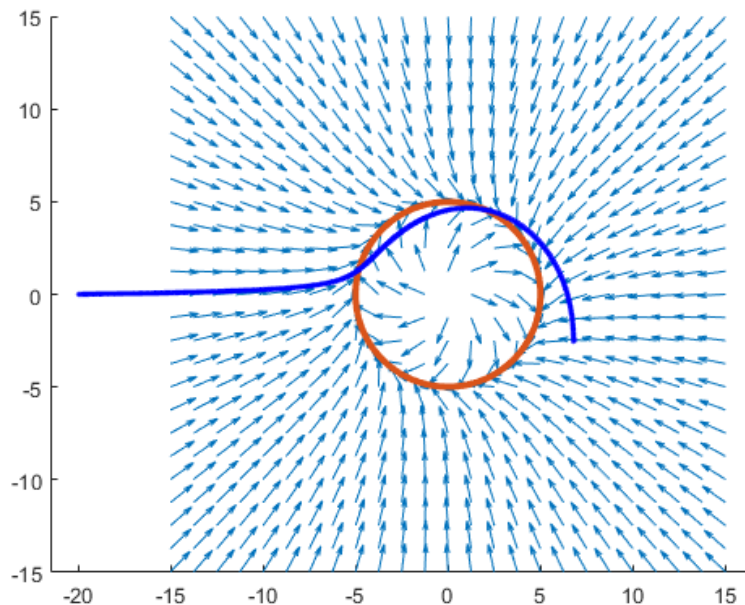


Figure 2.20: Dubins UAV actuator saturation

If the VF was adjusted earlier at an earlier state, the tracking error may be reduced. When using an obstacle, determining which direction the UAV must fly around the obstacle

is important to reduce distance flown. Determining functions for the sign and magnitude of the vector field weights to produce an optimal guidance.

2.4 Unmanned Aerial Vehicle Simulation

Testing new guidance, navigation, and control algorithms can be costly, require significant time, and requires an adequately large airspace. Ground stations need to be established which require power and shelter. Some small fixed wing UAVs may not be suitable to fly in all weather, therefore test flights may be canceled due to weather conditions. Lastly, larger UAVs need to have FAA clearance before flight which has to be pre-approved and takes time. Before spending the time to reserve airspace and allocate man hours for flight tests it is important to test algorithms in a controlled environment. One way to accomplish testing without actual flight is through validation through mobile robots simulating fixed wing constraints [18], [19], [20]. Programming a mobile robot, such as one shown in Figure

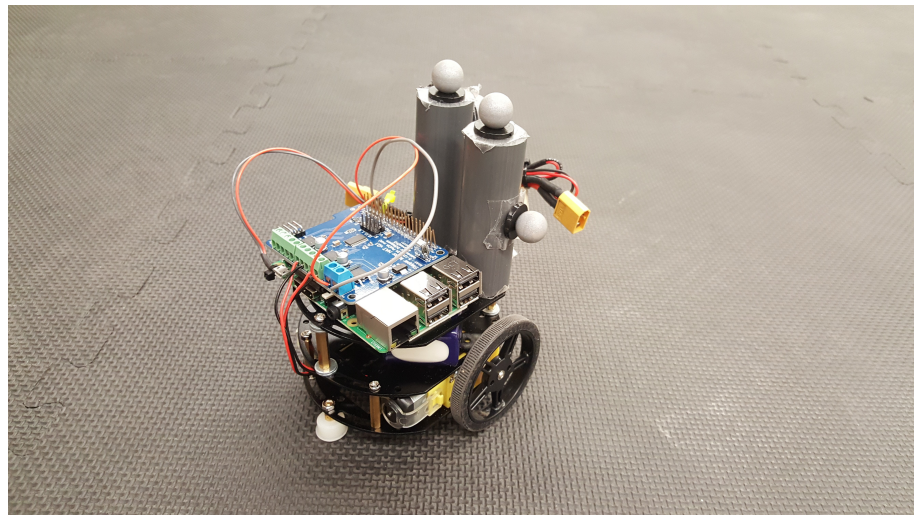


Figure 2.21: Differential drive mobile robot simulating fixed wing UAV Dubins constraints

2.5 Literature Review Summary

•

REFERENCES

- [1] Bone, E., “UAVs backbround and issues for congress.pdf,” 2003.
- [2] Sujit, P., Saripalli, S., and Sousa, J. B., “Unmanned Aerial Vehicle Path Following: A Survey and Analysis of Algorithms for Fixed-Wing Unmanned Aerial Vehicless,” *IEEE Control Systems*, Vol. 34, No. 1, Feb. 2014, pp. 42–59.
- [3] Beard, R. W. and McLain, T. W., *Small unmanned aircraft: theory and practice*, Princeton University Press, Princeton, N.J, 2012, OCLC: ocn724663112.
- [4] Khatib, O., “Real-time obstacle avoidance for manipulators and mobile robots,” *The international journal of robotics research*, Vol. 5, No. 1, 1986, pp. 90–98.
- [5] Liu, Y. and Zhao, Y., “A virtual-waypoint based artificial potential field method for UAV path planning,” *Guidance, Navigation and Control Conference (CGNCC), 2016 IEEE Chinese*, IEEE, 2016, pp. 949–953.
- [6] Rimon, E., “Exact Robot Navigation Using Artificial Potential Functions.pdf,” 1992.
- [7] Goerzen, C., Kong, Z., and Mettler, B., “A Survey of Motion Planning Algorithms from the Perspective of Autonomous UAV Guidance,” *Journal of Intelligent and Robotic Systems*, Vol. 57, No. 1-4, Jan. 2010, pp. 65–100.
- [8] Borenstein, J. and Koren, Y., “Real-time obstacle avoidance for fast mobile robots in cluttered environments,” *Robotics and Automation, 1990. Proceedings., 1990 IEEE International Conference on*, IEEE, 1990, pp. 572–577.
- [9] Borenstein, J. and Koren, Y., “The vector field histogram-fast obstacle avoidance for mobile robots,” *IEEE transactions on robotics and automation*, Vol. 7, No. 3, 1991, pp. 278–288.
- [10] Nelson, D. R., “Cooperative control of miniature air vehicles,” 2005.
- [11] Frew, E., “Lyapunov Guidance Vector Fields for Unmanned Aircraft Applications.pdf,” .
- [12] Frew, E. W., “Cooperative standoff tracking of uncertain moving targets using active robot networks,” *Robotics and Automation, 2007 IEEE International Conference on*, IEEE, 2007, pp. 3277–3282.
- [13] Chen, H., Chang, K., and Agate, C. S., “Tracking with UAV using tangent-plus-Lyapunov vector field guidance,” *Information Fusion, 2009. FUSION'09. 12th International Conference on*, IEEE, 2009, pp. 363–372.
- [14] Chen, H., Chang, K., and Agate, C. S., “UAV path planning with tangent-plus-Lyapunov vector field guidance and obstacle avoidance,” *IEEE Transactions on Aerospace and Electronic Systems*, Vol. 49, No. 2, 2013, pp. 840–856.

- [15] Md, Z., Rg, C., and Dj, G., "Simplex Solutions for Optimal Control Flight Paths in Urban Environments," *Journal of Aeronautics & Aerospace Engineering*, Vol. 06, No. 03, 2017.
- [16] Pimenta, L. C., Pereira, G. A., and Mesquita, R. C., "Fully continuous vector fields for mobile robot navigation on sequences of discrete triangular regions," *Robotics and Automation, 2007 IEEE International Conference on*, IEEE, 2007, pp. 1992–1997.
- [17] Goncalves, V. M., Pimenta, L. C. A., Maia, C. A., and Pereira, G. A. S., "Artificial vector fields for robot convergence and circulation of time-varying curves in n-dimensional spaces," IEEE, 2009, pp. 2012–2017.
- [18] Ren, W., McLain, T., Sun, J.-S., and Beard, R., "Experimental validation of an autonomous control system on a mobile robot platform," *IET Control Theory & Applications*, Vol. 1, No. 6, Nov. 2007, pp. 1621–1629.
- [19] Louali, R., Djouadi, M. S., Nemra, A., Bouaziz, S., and Elouardi, A., "Designing embedded systems for fixed-wing UAVs: Dynamic models study for the choice of an emulation vehicle," IEEE, Feb. 2014, pp. 1–6.
- [20] Louali, R., Elouardi, A., Bouaziz, S., and Djouadi, M. S., "Experimental Approach for Evaluating an UAV COTS-Based Embedded Sensors System," *Journal of Intelligent & Robotic Systems*, Vol. 83, No. 2, Aug. 2016, pp. 289–313.